Electroencephalography (EEG)-Based Brain–Computer Interface (BCI): A 2-D Virtual Wheelchair Control Based on Event-Related Desynchronization/Synchronization and State Control

Dandan Huang, *Member, IEEE*, Kai Qian, Ding-Yu Fei, *Member, IEEE*, Wenchuan Jia, Xuedong Chen, and Ou Bai

***Abstract*—This study aims to propose an effective and practical paradigm for a brain–computer interface (BCI)-based 2-D virtual wheelchair control. The paradigm was based on the multi-class discrimination of spatiotemporally distinguishable phenomenon of event-related desynchronization/synchronization (ERD/ERS) in electroencephalogram signals associated with motor execution/imagery of right/left hand movement. Comparing with traditional method using ERD only, where bilateral ERDs appear during left/right hand mental tasks, the 2-D control exhibited high accuracy within a short time, as incorporating ERS into the paradigm hypothetically enhanced the spatiotemoral feature contrast of ERS versus ERD. We also expected users to experience ease of control by including a noncontrol state. In this study, the control command was sent discretely whereas the virtual wheelchair was moving continuously. We tested five healthy subjects in a single visit with two sessions, i.e., motor execution and motor imagery. Each session included a 20 min calibration and two sets of games that were less than 30 min. Average target hit rate was as high as 98.4% with motor imagery. Every subject achieved 100% hit rate in the second set of wheelchair control games. The average time to hit a target 10 m away was about 59 s, with 39 s for the best set. The superior control performance in subjects without intensive BCI training suggested a practical wheelchair control paradigm for BCI users.**

***Index Terms*—Brain–computer interface (BCI), electroencephalogram (EEG), event-related desynchronization, event-related synchronization, two-dimensional (2-D), wheelchair control.**

I. Introduction

RESEARCH on brain–computer interfaces (BCIs) has approximately 40 years during which time the potential of BCI applications has been explored in many fields, including: communication, robotics, and mobility control, and neuroprosthetics [1]–[7]. The BCI translates intentions directly into machinery commands, bypassing the conventional neural muscular conduction pathway in the human body [8]. This enables patients with paralysis to regain independence, improve their quality of life [9]–[11], and potentially reduce the great economic cost caused by the continuous needs of care givers [12].

Our group has been working on electroencephalography (EEG)-based BCIs aiming at developing 2-D control BCIs [13]–[15] for potential applications such as wheelchair control. With such BCIs the users should be able to control the wheelchair at their own pace and the control is quickly attained. To that end, users learn how to voluntarily modulate the different oscillatory rhythms through execution of physical or imagined motor tasks and quickly develop control of the BCI. To facilitate the learning process, we rely on both machine learning techniques to train/select effective classifiers that yield high classification accuracies using subject-specific EEG features [16] and incorporating new physiological features to essentially enhance the difference/separability between patterns generated by mental tasks [15].

One of the main challenges of EEG-based BCI is insufficient decoding accuracy due to the low signal-to-noise ratio (SNR) of EEG signals, which are generated by synchronous activity of millions of cortical neurons. As EEG signals are detected from electrodes on the scalp, spatial resolution is reduced while the noise level is increased. This has motivated the BCI research groups to seek reliable features and advanced strategies to best overcome the low SNR so as to build a system of sufficient reliability and ease of use. The most commonly used feature in cursor or wheelchair control is event-related desynchronization (ERD) [17], a phenomenon of EEG amplitude attenuation during mental tasks indicating cortical activation. Through motor imagery of hand/foot movements by detecting spatially different ERD patterns, or through regulating brain rhythms to decrease signal variability and increase SNR in order to discriminate control state ERD from noncontrol state baseline activity, users could achieve 1-D, 2-D cursor or wheelchair control [6], [18]–[23]. Recently, 3-D virtual helicopter control game [24] using intelligent control strategies [6], [23], [25]–[27] was reported, and 3-D wheelchair cursor control through right/left hand and foot motor imagery after a series of training sessions [28] has also been achieved. However, such kinds of methods usually require intensive user training [29], in which case fatigue may affect performance in long-term use, especially when

Manuscript received July 25, 2011; revised February 21, 2012; accepted February 25, 2012. Date of publication April 05, 2012; date of current version May 18, 2012.

D. Huang, K. Qian, D.-Y. Fei, and O. Bai are with the Department of Biomedical Engineering, Virginia Commonwealth University, Richmond, VA 843067 USA (e-mail: huangd2@vcu.edu; kqian@iit.edu; fei@vcu.edu; obai@vcu.edu).

W. Jia and X. Chen are with the State Key Laboratory of Digital Manufacturing Equipment and Technology, School of Mechanical Science and Engineering, Huazhong University of Science and Technology, Hubei 430074, China (e-mail: lovvchris@shu.edu.cn; chenxd@mail.hust.edu.cn).

Digital Object Identifier 10.1109/TNSRE.2012.2190299

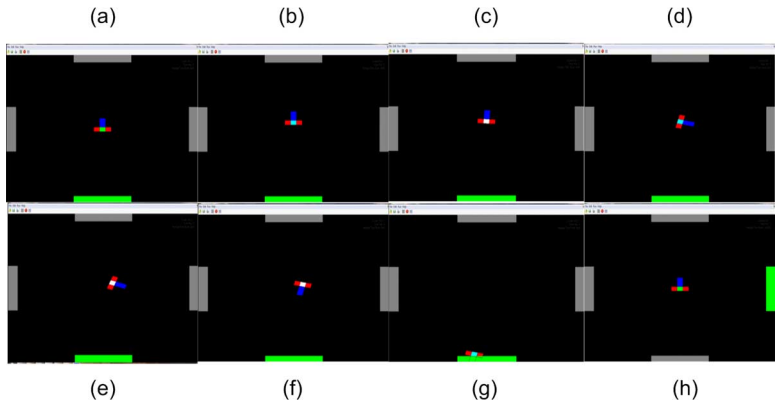

Fig. 1. Screen shots of virtual wheelchair control in one run. (a) Wheelchair started at the center of the screen-Stop State. (b) Wheelchair started to move upward along the blue bar direction after receiving Go/Stop Command-Running State. (c) Wheelchair started to make right turn after receiving Right Turn Command-Rotating State. (d) Wheelchair stopped rotating and started to move along blue bar direction after receiving Go/Stop Command-Running State. (e) Wheelchair stopped moving and started to make right turn after receiving Right Turn Command-Rotating State. (f) Wheelchair stopped rotating and started to move along blue bar direction after receiving Go/Stop Command-Running State. (g) Wheelchair reached the target-Stop State. (h) Simulation of wheelchair control restarted-Stop State.

the end users might be, for instance, severely paralyzed or ALS patients who suffer from both physical and mental weakness [30], [31]. Approaches detecting only ERDs with left/right hand motor execution/imagery may experience insufficient decoding accuracy as there is evidence that during unilateral hand movement, ERD starts contralateral to the side of movement about 2 s before movement onset and becomes bilateral at the time of movement onset [32]–[34]. In our previous study, bilateral ERDs were also observed [15], which potentially increased the difficulty in separating left hand and right hand mental tasks. Given that low detection error is more desirable in wheelchair control compared to applications in cursor control or computer games where speed is of higher importance and error tolerance is high, two questions arise; Is it possible to utilize new EEG features that may essentially provide higher separability among different mental tasks? How can a simple but effective paradigm enhance the control accuracy and contribute in a fast attained 2-D BCI for potential wheelchair control?

Our previous study [15] presented a feasible 2-D discrete control paradigm by incorporating a new feature, i.e., event-related synchronization (ERS) with cessation of imagined right/left hand movement. As ERS is spatially more focal on the contralateral hemisphere and the difference between ERS and ERD is greater than that of ERD and baseline activity used extensively in the conventional BCI systems, the detection of ERS might potentially be more reliable and result in higher decoding accuracy [35]. In this paper, we further improved the paradigm towards a continuous virtual wheelchair control BCI in three aspects. 1) To avoid bilateral ERDs with both hands' mental tasks, we designed three commands for 2-D control, one associated with right hand ERD, one with right hand ERS and one with left hand ERS. As will be explained in the method and result sections, this essentially enhanced decoding accuracy and thus ease of use. 2) Noncontrol state was incorporated to allow more control freedom. 3) A continuous wheelchair control strategy was carried out with reasonable control speed within the normal range of wheelchair speed.

II. Method

A. Subject

Five right-handed healthy subjects (S1–S5, two females and three males) age 23–30 participated in this study. S2 had 6 hours BCI experience half a year ago for another irrelevant study; S1, S3–S5 had no previous BCI experience. All the subjects were participating for the first time in this study, and gave informed consent. The protocol was approved by the Institutional Review Board.

B. Data Recording

EEG was recorded from 27 (tin) surface electrodes (F3, F7, C3A, C1, C3, C5, T3, C3P, P3, T5, F4, F8, C4A, C2, C4, C6, T4, C4P, P4, T6, FPZ, FZ, FCZ, CZ, CZP, PZ, and OZ) attached on an elastic cap (Electro-Cap International, Inc., Eaton, OH) according to the international 10–20 system [36], with reference from the right ear lobe and ground from the forehead. Two surface electromyography (EMG) electrodes were taped over the right and left wrist extensors, used to monitor the hand movement. Electrodes for bipolar electrooculogram (EOG) above left eye and below right eye were also pasted. Total duration of preparation for obtaining consent, explaining paradigm, and setting up electrodes took around 30 min to 1 h. Signals from all the channels were amplified (g.tec GmgH, Schiedlberg, Austria), filtered (0.1–100 Hz) and digitized (sampling frequency was 256 Hz). All impedances were kept below 5 kΩ. The digital signal was processed online using a custom-made MATLAB (MathWorks, Natick, MA) Toolbox: BCI to virtual reality or BCI2VR [13], [16]. The BCI2VR programs provided both the visual stimulus for the calibration and the 2-D wheelchair-control game, as well as online processing of the EEG signal.

C. Experimental Paradigm

1) Online Wheelchair Control Paradigm: Fig. 1 shows the small screen images which demonstrate a sequence of steps in one run. The converted real size of the simulated scenario was $20 \times 20\ \mathrm{m}^2$. The relative sizes of the targets on all four sides were

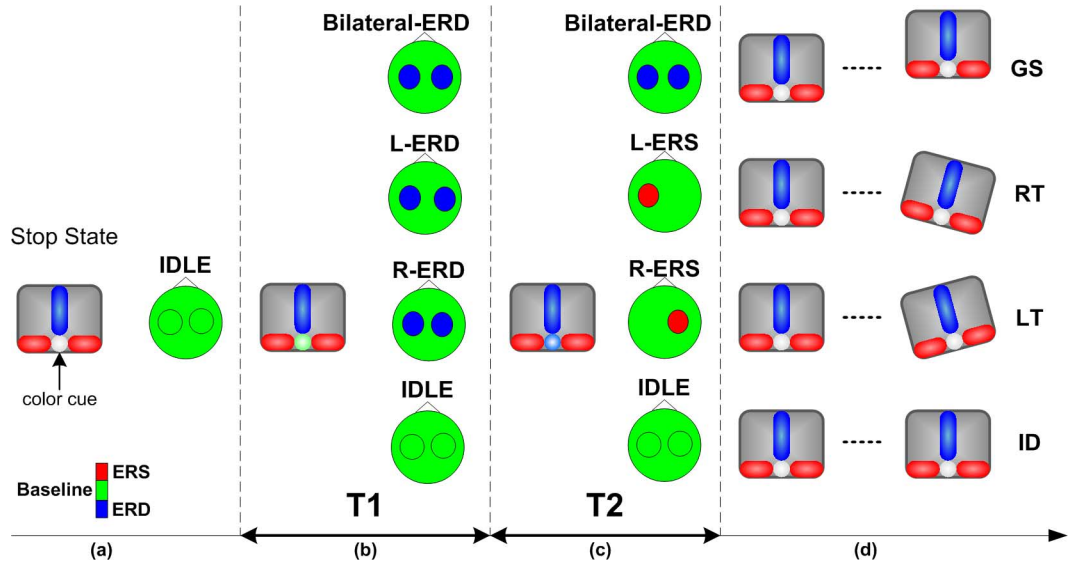

Fig. 2. Strategy of wheelchair control. (a)–(d) Follow the time sequence. (a) In stop state, the wheelchair is keeping still. (b) In the first cue period T1, subjects start any of the motor tasks; from top to bottom are the four situations: right wrist extension-left hemisphere ERD pattern, right wrist extension-left hemisphere ERD pattern, left wrist extension-right hemisphere ERD pattern or no motor task-Idle/baseline activity. (c) In the second cue period T2, subjects continue with the task: continue right wrist extension-left hemisphere ERD pattern, stop right wrist extension and relax-left hemisphere ERS, stop left wrist extension and relax-right hemisphere ERS, or no motor task-baseline activity. (d) Movement intention is decoded and wheelchair is driven to move forward (or stop when moving), turn right, turn left or keep current moving status. Inter-trial interval (the end of T2 to the beginning of next T1) is 2 s.

TABLE I
WHEELCHAIR CONTROL COMMANDS, ASSOCIATED MOTOR TASKS, DETECTED EEG PATTERNS, AND OUTPUT CONTROL ACTIONS

Control Command	Associated Motor Task		Detected Activity in T2	Control Actions	
	T1	T2		Current State	Next State
Go/Stop	Right wrist extension	Continued right wrist extension	Bilateral ERD	Stop	Running
				Running	Stop
				Rotating	Running
Right Turn	Right wrist extension	Relaxation	Left hemisphere ERS	Stop	Rotating
				Running	Rotating
Left Turn	Left wrist extension	Relaxation	Right hemisphere ERS	Stop	Rotating
				Running	Rotating
Idle State	No motor task	No motor task	Idle/resting activity	Any state	Unchanged

6×1 m^2. Each run began with the wheelchair at the center, and terminated when the wheelchair either hit the target (success) or at any time hit the edge elsewhere (failure). Subjects could inform the investigator to stop the experiment at any time, and the investigator monitored the signal quality and EMG activity throughout the experimental procedure. The wheelchair moving speed was set to 0.4 m/s, with a rotating speed 27 s/360°, within common wheelchair speeds [37]. The wheelchair could move forward only in the direction of the blue bar, which always faced upwards at the beginning of each run. The wheelchair rotated with the square in its center as the axis. The square also served as the color cue; its color changes synchronized with the external auditory cues in different frequencies, reminding subjects of different task periods. Section II-C2 explains in detail how the wheelchair was controlled by performing mental tasks and the EEG patterns that were expected to be exhibited along with the tasks.

2) Wheelchair Control Strategy: Fig. 2 shows the EEG power changes with execution of four mental tasks separately (in four rows). The performing of each task together with expected EEG power changes and output control command is summarized in Table I, and visualized in Fig. 2. Take the top row for example. This is a "Go/Stop" command. Task began with the T1 time window (0–1.5 s), indicated by the color changes of the color cue (the square in the center of the wheelchair changing to green) which occurred simultaneously with the first auditory cue onset. When this happened, subjects performed right wrist extension or motor imagery (refer Table I). When the color cue changed to blue, T2 time window (1.5–4 s) began and subject heard the second auditory cue. In this period, subjects continued performing right wrist extension or motor imagery until the end of T2 window, when the color cue changed to white and the third auditory cue onset. Movement intention was decoded and control action was taken.

Specifically.

1) Go/Stop Command ("GS"): bilateral ERD in both T1 and T2 windows, i.e., when users want the wheelchair to move forward, or stop when it is moving, they perform (imagined) right wrist extension in both T1 and T2 windows. This command will make one of the following three possible state changes.

a) Switch from Stop State to Running State, wheelchair will start moving.
b) Switch from Running State to Stop State, wheelchair will stop moving.
c) Switch from Rotating State to Running State, wheelchair will stop rotating and start to move.

2) Right Turn Command ("RT"): bilateral ERD in T1 window and ERS on the left hemisphere in T2 window, i.e., when users want to make a right turn, they perform (imagined) right wrist extension in T1 window and stop the (imagined) movement at the beginning of T2 window. This command will make the following state change.
   a) Switch from Stop State or Running State to Rotating State, wheelchair will start to rotate to right.
3) Left Turn Command ("LT"): bilateral ERD in T1 window and ERS on the right hemisphere in T2 window, i.e., when users want to make a left turn, they perform (imagined) left wrist extension in T1 window and stop the (imagined) movement at the beginning of T2 window. This command will make the following state change.
   a) Switch from Stop State or Running State to Rotating State, wheelchair will start to rotate to left.

The Idle ("ID")/noncontrol state is the natural state when subjects do not want to change moving state; whenever the computer detects "ID" state, no control command will be sent out and thus the wheelchair keeps its current state. The involvement of "ID" state in this study renders the continuous control and makes the control process easier.

D. Experiment Procedure and Signal Processing for Decoding Movement Intention

For either physical or motor imagery session, each subject performed 25 min of calibration, containing 96 "ID" tasks and 32 each of the other tasks ("GS," "RT," "LT"), with a 5 min break in the middle. This created models based on which subject performed two sets of online wheelchair control games, each set had eight runs/target reaching, two for each target location, with targets showing up pseudo-randomly. One to 5 min breaks were given in between games or runs.

1) Spatiotemporal Filtering and Feature Selection: The online data were processed through three steps to decode the movement intention: 1) spatial filtering, 2) temporal filtering, and 3) feature selection and classification.

Surface Laplacian derivation (SLD) was applied as the spatial filter, where EEG signal from each electrode was referenced to the averaged potentials from the nearby four orthogonal electrodes [38]. SLD operation improves the localization of sources [39], enhance the EEG feature of local synchrony, i.e., frequency power changes [40], so that the spatial difference of different hand motor tasks would be more distinguishable.

Temporal filtering was done through the power spectral density estimation of the spatially filtered EEG signal in the T1 and T2 window. According to the visual inspection of time-frequency plots of ERD and ERS after the calibration session, one period from T1 and one period from T2 were extracted in order to obtain the strongest ERD/ERS; each subject could have different extraction periods. Due to the nonstationary property of the signal [15], the Welch method with a Hamming window was applied to reduce estimation variance and side-lobe effect [41]. To keep consistence, we continued using 4 Hz frequency resolution or a segment length of $256/4 = 64$ under 50% overlapping, which exhibited the optimal results in our previous studies [15], [16].

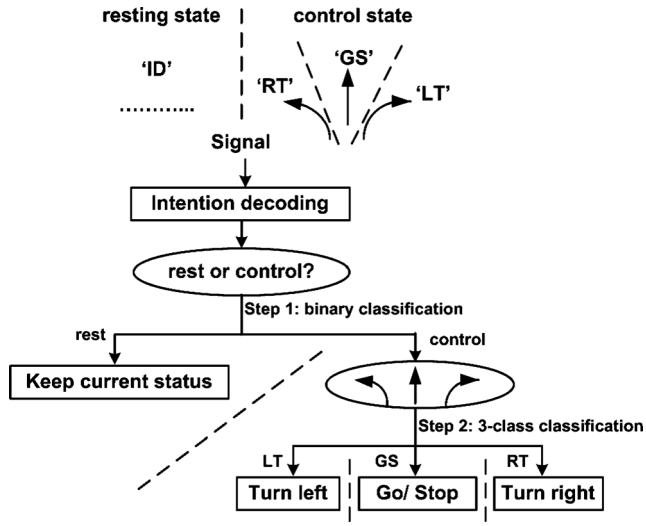

Fig. 3. Demonstration for the two-step classification. Step 1 is a binary classifier, separating Idle from Active; Step 2 is three-class classifier, further determine which Active command the sample belonged to.

Assuming that movement intention associated cortical activities occur over the motor cortex, we empirically reduced the channel number from 29 to 16, which covered both left and right motor areas (channels CZA, C3A, CZ, C1, C3, C5, CZP, C3P, PZ, P3, C4A, C2, C4, C6, C4P, P4). Furthermore, we extracted alpha and beta band (8–30 Hz) activities for modeling and classification. Consequently, the total number of extracted features was 8 (frequency bins) $\times$ 16 (channels) $=128$ features. Bhattacharyya distance provides an index of feature separability for binary classification, which is proportional to the inter-class mean difference divided by intra-class variance [42]. The empirically extracted features were ranked by the Bhattacharyya distance for further classification.

2) Two-Step Modeling/Classification: As Fig. 3 shows, in this study, we designed a two-step classification. The first step was to identify whether the signal belonged to control commands (true positive or TP) or noncontrol commands (true negative or TN), as we wanted to keep false triggering/false positive rate (FPR) as low as possible and true positive rate (TPR) sufficiently high. For modeling using the calibration dataset, we first grouped all three active tasks ("GS," "RT," "LT") into one category as control signals, leaving "ID" tasks as another category, i.e., noncontrol signals. We applied Mahalanobis linear distance (MLD) classifier to find the prototype centers of the two categories. For each sample, we calculated the distance between itself and each center and then took the difference $\Delta\ \vec{d}$ to finally get $\Delta\ \vec{d}$ for all samples. By applying a series of thresholds to separate $\Delta\ \vec{d}$, we could classify the samples under different accuracies, we then got the ROC plot [43] for all thresholds. We selected an optimal threshold under which FPR was lower than 10% and TPR higher than 80%, or suboptimal threshold which

TABLE II
HIT RATE AND AVERAGE TARGET HIT DURATION IN EACH GAME

Hit rate (%) & Duration (s)	physical		imaginary	
	Game1(8 runs)	Game2 (8 runs)	Game 1 (8 runs)	Game 2 (8 runs)
S1	100 (85.8)	87.5 (52.0)	*	*
S2	100 (40.8)	100 (34.8)	100 (43.0)	100 (41.5)
S3	100 (63.3)	100 (63.0)	100 (59.5)	100 (39.5)
S4	87.5 (67.0)	100 (58.0)	87.5 (70.9)	100 (88.0)
S5	100 (50.5)	100 (49.8)	100 (75.3)	100 (65.5)

was close to the left upper corner of the ROC curve and applied that threshold in the online wheelchair control to separate Idle from Active. If it was Idle, the computer did not send out any control command, instead, the wheelchair kept current moving; if classified to Active, the second step was a three-class classification, to further determine whether it was a "GS," "LT," or "RT" command. In each step, the features (power data extracted from T1 and T2 windows over different frequency bins and electrode locations) were ranked by the Bhattacharyya distance and the ones with higher ranks were used for classification by a MLD classifier.

III. RESULT

Table II shows that except for S1 who quit due to sleepiness, the other four subjects who finished all physical and imagery sessions finally got 100% target hit rate in the second set of games (Game 2) with motor imagery, with time generally shorter than Game 1 (except for S4), due to fewer misdetections in Game 2. This shows that subjects became familiarized with the BCI operation and learnt to cooperate with the BCI system and improve their sense of kinesthetic imaginary. Notice that Game 2 in the physical session also took a shorter time than that in Game 1 ($t = 5.03, \mathrm{df} = 39, p-\mathrm{value} < 0.001^*$), which can be considered evidence that the subjects started to learn.

Taking a closer look at the target reaching time in the second imaginary game, we found that 58.6 s was the average time for subject 2, 3, 4, and 5 to reach a target 10 m away. 5.9 s/m reflected a reasonable speed for a wheelchair used by paralyzed patients [37].

Both binary and three-class classification affected subjects' control performance; binary classification was of more importance as noncontrol states (Idle tasks) accounted for 46.9% of all tasks. This was in accordance with another study conducted by Pfurtscheller's group [44] where the subject "walked" straight in a virtual environment using two signals, intentional control (IC) and noncontrol (NC) in order to reach avatars. As they pointed the drawback of their design was that the subject was forced

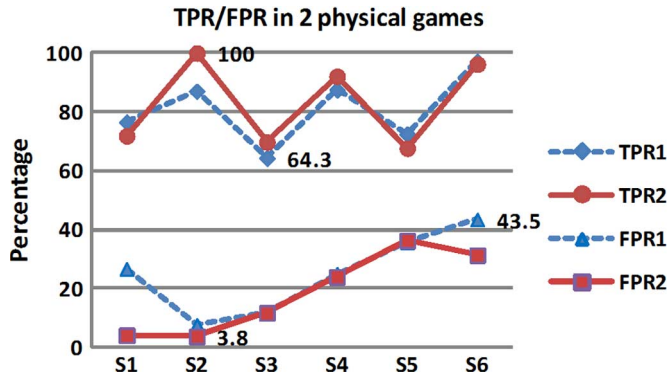

Fig. 4. True positive rate (TPR or active command recognition rate), and false positive rate (FPR or the ratio of "Idle" command recognized as active command) for all subjects in two physical games.

to stop at the avatar for a minimum 1 s NC period, but the actual subjects' stopping time was very short with the mean 0.47 s, which means the false triggering (FP) was inevitable. In our imaginary movement, no values for TP and FP can be given, for the same reason as the study mentioned above. Using their evaluation method, for S2, S3, S4, and S5, TPR in motor imagery would be $63/64 = 98.4\%$ and missed hits (false negative rate/FNR) $=1/64 = 1.6\%$ (calculated from Table II); FP and true negative (TN) cannot be evaluated. However, since target reaching time for motor imagery was comparable to that for physical movement, we can calculate TPR and FPR (shown in Fig. 4) by monitoring the EMG activity in physical movement.

TPR is the sensitivity, indicating the active command recognition rate. For all subjects, TPR ranged from 64.3% to 100% (mean 84.3%) which was much higher than chance value 53.1% (percentage of active command). FPR is the false triggering rate ranging from 3.8% to 43.5% (mean 19.0%) which means specificity (TNR or 1-FPR) was much higher than chance value 53.1% (percentage of active command). FPR is the false triggering rate ranging from 3.8% to 43.5% (mean 19.0%) which means specificity (TNR or 1-FPR) was 81.0%, much higher than chance value 1%–53.1% or 46.9%. For physical movement, average target hit time was 56.5 s, obtained from Table II. With the calculation above, one run took about 9.5 commands to hit the target, about 0.89 Idle was detected as active (1 false triggering) and $(5.31 - 4.48 = 0.83)$ active commands were detected as Idle (1 insensitivity). This calculation gave us a general idea for motor imagery control which took an average 60.4 s for each target hitting. Under this detection rate, subjects reported good sense of control.

Fig. 5 shows the traces for all the games in physical and imaginary sessions for each subject. We can see that S2, with several hours' previous exposure to other BCI studies, was more comfortable than the other subjects even from the first run and also displayed good performance in motor imagery. S3, although a naive BCI user, caught up very quickly and over performed S2 in the last motor imagery game.

Table III shows the best EEG features used for each subject in physical and binary wheelchair control games, in terms of electrodes and frequency bins (4 Hz bin width). We notice that frequency bins for binary classification more often appeared in alpha and lower beta bands (bin 3–6 or 9–24 Hz); for three-class

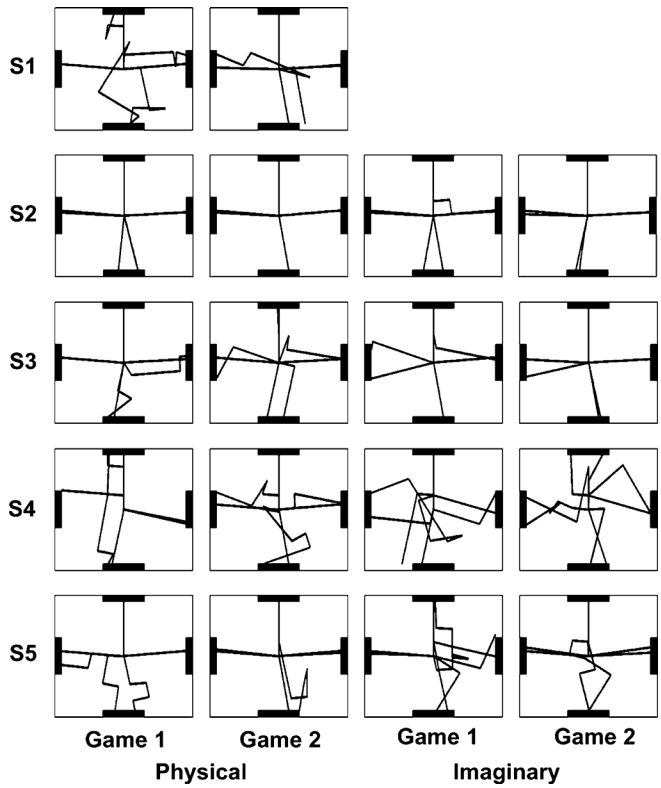

Fig. 5. Traces of all physical and motor imagery games for each subject. Each game had eight runs/target reaching.

TABLE III
EEG FEATURES (SPECIFIC FREQUENCY BINS AT SPECIFIC ELECTRODES) THAT WERE USED FOR BINARY CLASSIFICATION (IDLE/ACTIVE) AND THREE-CLASS CLASSIFICATION (GS/RT/LT) IN PHYSICAL/MOTOR IMAGERY SESSION FOR EACH USER

	Electrode (frequency bin)			
	Physical		Imaginary	
User	Binary	3-class	Binary	3-class
S1	C3,C4	C3,C4	C3,C4	C3,C4
	(5,6)	(5,6)	(4,5)	(4,5)
S2	C3	C3,C4	C3	C3,C4
	(5,6)	(4,5)	(5,6)	(3,4)
S3	C3,C4	C1,C3	C3,C4	C1,C3
	(6,7)	(7,8)	(4,5)	(7,8)
S4	C3,C3P	C3,C4	C3,C3P	C3,C4
	(5,6)	(6,7,8)	(4,5)	(6,7)
S5	C3,C4	C1,C4	C3,C4	C1,C2
	(4,5)	(6,7,8)	(4,5)	(7,8)

classification, bin 7 and 8 (25–32 Hz) were involved more often. This proved the fact that for 3-class classification, ERS, which occurred mostly in beta band, played a significant role. The best channels for binary classification more often appeared in C3 and C4; for 3-class classification, channel C1 and C2 were also involved for some subjects, which may indicate that ERS in central motor area was stronger for some subjects and its contrast with ERD contributed much in discrimination of GS/RT/LT.

Fig. 6 is an illustration showing the ERD/ERS of S2 and S3 in motor imagery. Best electrodes were selected (C3 and C4 for S2, C1 and C4 for S3). As can be seen, during the Idle state, subjects thought about nothing, baseline activity exhibited throughout all frequency bands. In 0–1.5 s of the active tasks where subjects imagined wrist extensions, ERD (blue) occurred most of the time, at around 10–20 Hz frequency band, bilaterally distributed. During 1.5–4 s, subjects either continued imagined movement where ERD still sustained or stopped motor imagery where ERS (red) showed up. ERS occurred mainly on the contralateral hemisphere. For S3, ERS appeared at higher frequency band than S2, and more towards central electrodes. From the plots we can see that the spatial and temporal EEG signal differences among different motor tasks can be reflected from ERD/ERS patterns associated with movement intention which can be decoded by analyzing the data in T1 and T2 time windows.

To answer why involving ERS as opposed to ERD could potentially enhance detection accuracy, we need to quantitatively examine ERD/ERS in the three mental tasks. Fig. 7 shows ERD/ERS values at C3 and C4 for S2–S5 in physical movement (top two) and imagined movement (bottom two), under the left turn (LT), right turn (RT) or Go/Stop (GS) tasks. The left side describes the T1 window and right side describes the T2 window. First, it is obvious that ERD/ERS power distribution in the physical and motor imagery sessions are quite similar, except that power in motor imagery session is much weaker than that in physical session, which is consistent with our previous reports. Second, as we can see in the T1 window (Fig. 7), for all three tasks, both C3 and C4 generally exhibit negative values because of the bilateral ERD distribution during left/right hand (imagined) movement. Conventional rhythmic regulation is largely based on an ERD approach, however, due to the fact that ERD could be difficult to be detected from baseline because of the variance and the similarity that exists among different mental tasks (p-value$= 0.8227$ for physical and p-value $= 0.5207$ for motor imagery), intensive training may be necessary before stable control could be attained. In contrast, the proposed novel design makes the most of spatial and temporal difference of EEG features during mental tasks, as it involves spatially focal ERS associated with cessation of mental tasks in the T2 window, which essentially enhances the difference among mental tasks. As can be seen in the T2 window, positive power values generally exhibit on the contralateral hemisphere for RT and LT tasks while, in contrast, negative power values bilaterally exhibit for GS tasks. Three tasks can be classified easily in the physical session (p-value $= 0.0002^{*}$) and less easily in the motor imagery session (p-value$= 0.0856$).

For each subject, the best electrode locations and frequency bins used for control signals were provided by Bhattacharyya distance. Fig. 8 is an example where Bhattacharyya distance was used in binary classification to separate active tasks from Idle. One of the best frequency bins were selected to illustrate each subject's performance. As subjects exhibited variant performances in motor tasks, we usually selected two or three major channels/frequency bins for each subject as the best ones. As can be seen, S2 was more familiar with BCI than the other three, and therefore the pattern was more stable (less noisy in the sur-

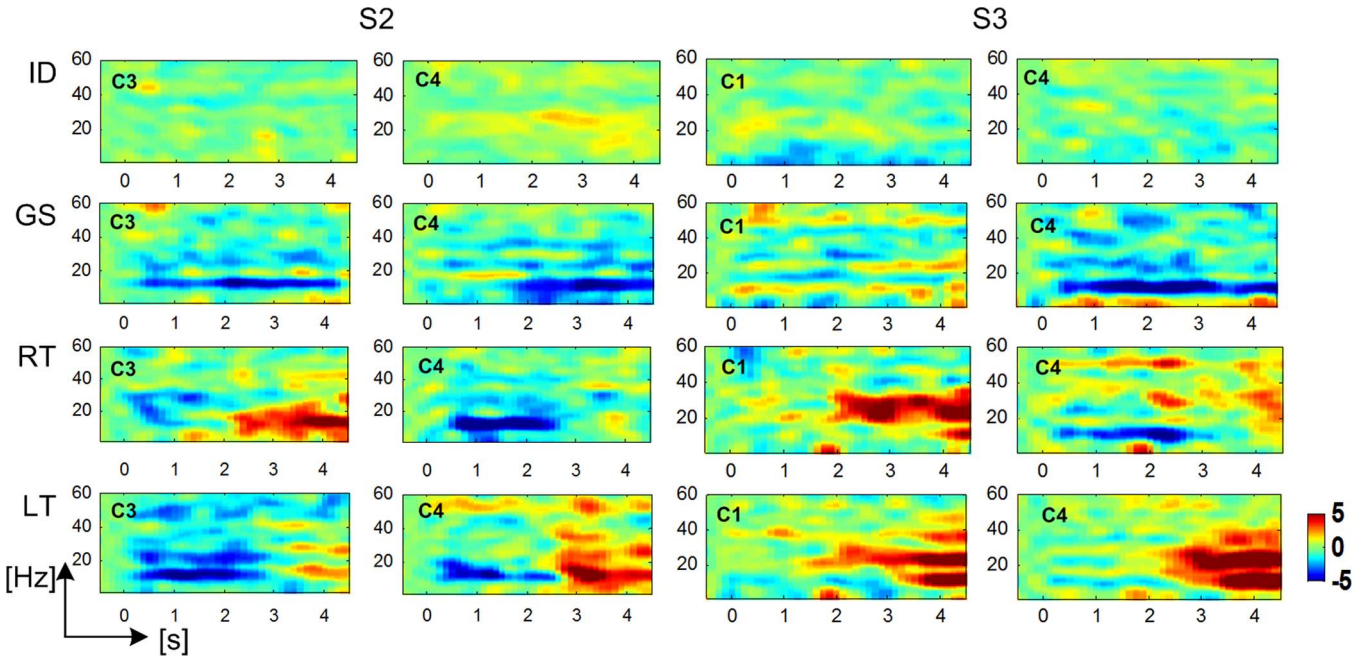

Fig. 6. Illustration of time-frequency plots for S2 and S3 in motor imagery tasks. X axis represents time. Specifically, in non-Idle tasks, from 0–1.5 s subjects performed imagined right wrist extension (GS/RT) or left wrist extension (LT) and from 1.5–4 s, either continued imagined extension (GS) or stopped and relaxed (RT/LT). Y axis indicates frequency. Red means power increase and blue is power decrease, with green the baseline.

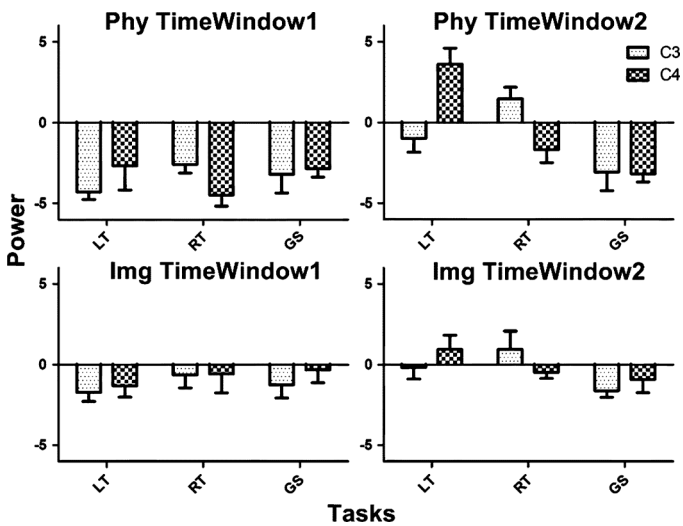

Fig. 7. ERD/ERS amplitude at C3 and C4 for subject S2–S5 in physical movement (top two) and imagined movement (bottom two). Left side describes T1 window and right side describes T2 window.

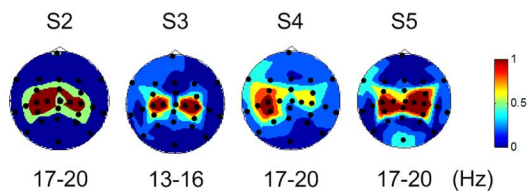

Fig. 8. Head topography plots of Bhattacharyya distance for binary discrimination for the four subjects in motor imagery tasks. Dark red areas indicate highly distinguishable and dark blue means the opposite. Best frequency bins and channels for each subject differ.

rounding electrodes) than others. Compared with S2, S3 had the best electrodes more focal, evenly on both hemispheres. S4 had C3 and C3P both on the left hemisphere, as the best electrodes for binary classification and S5 had a few ideal electrodes providing good separability, similar with S2.

IV. Discussion

In this paper, we have presented an effective and practical paradigm of a continuous EEG-based BCI for virtual wheelchair control of subjects in their first visit. The wheelchair could be operated to turn left or right, to go straight or stop, with all the basic motion functions that a real wheelchair has. The prominent induced power decrease (ERD) and power increase (ERS) associated with imagined natural movements allowed the reliable discrimination of movement intentions, and therefore improved control accuracy and increased the degrees of freedom of the wheelchair control system. The result showed that a high hit rate (87.5%–100%) could be achieved by controlling the simulated wheelchair continuously moving in a 2-D plane when subjects imagined hands' movements. It should be noted that subjects achieved the reasonable control performance in their first visits.

Compromise is always needed when optimizing control accuracy and speed. While control accuracy is satisfying, increasing the wheelchair's movement and rotation speed is also of key interest. As we have noticed, it took time for the correction of wheelchair overshoot which can be observed in Fig. 5 from the sharp turn of the trajectories. This was caused by the unresponsive detection periods T1 and T2. However, as T1 and T2 are essential for ERD and ERS to happen, they are indispensable for the proposed strategy. Thus, to optimize the length of the detection window to make a more flexible, yet reliable wheelchair control is our next step.

Moreover, reduction of the number of electrodes could be performed with the expectation of comparable results, as we found

through analysis that subjects exhibited stable features in several electrodes, namely C1–C4, and occasionally C3P and C4P. Fewer electrodes would reduce setup time and undoubtedly will aid the spirit of the subjects. As this was the subjects' first visit, we asked them to perform physical movement first. On one hand, it allowed us to examine their movement execution and ERD/ERS features before motor imagery and on the other hand it allowed them to find the right way to perform motor imagery tasks.

EMG contamination from facial muscles may possibly cause serious problems in BCI development [45]. Throughout the experiment, EMG signal was monitored for all subjects, to make sure correct movements were performed and no EMG occurred during motor imagery. Further, feature analysis showed that beta activities restricted to motor areas were used for classification. Therefore, EMG contamination was not a concern in this study.

Compared with our previous study where users performed step-by-step discrete 2-D cursor control, which is stable but slow, the current study is taking a major step forward in trying to apply the rationale to wheelchair control, by involving noncontrol state and continuous control strategy as a part of our user friendly design. Specifically, subjects imagined human natural hand movements. Imagined left hand movement in T1 window sent out control command for left turn; imagined right hand movement in T1 window sent out control command for right turn; imagined right hand movement in both T1 and T2 window sent out Go/Stop command. It is in a manner similar to driving, when people want to start the engine, finish turning and go straight, or stop during emergency, they step firmly on the accelerator or brake for a period. Drivers hold this state when they don't want to change direction or stop, which is similar to the noncontrol state in this study where subject remained relaxed. This gave subjects 2–4.5 s intervals between two active commands which allowed them to take a break and get prepared for the next movement. For the condition that they kept moving/turning, the noncontrol state allowed even longer relaxation time for the subjects, or for the potential paralyzed patients. The current design aimed at ease of use for the potential user while keeping a reliable sense of control, with good control speed.

Another aspect of user friendly design is that the paradigm fixed the initial facing direction of the wheelchair upwards in each run while changing target directions, in order to mimic the real world target reaching tasks, where users may need to turn the wheelchair by different angles and then move forward. In the typical setting as we did here: moving forward, turning left/right and to the opposite directions, we had a good chance of examining all combinations of commands, such as noncontrol and control, move forward and stop, turn and move forward, just as in real wheelchair control or car operation. Yet, the current virtual wheelchair design is adopted to be most user friendly in a virtual scenario. Once the approach is fully validated and the system performance is optimized in a virtual environment, the next step of the experiment will be taken. Before a real wheelchair can be finally incorporated into the system, integration issues should be carefully considered and simulated, parameters such as mechanical system delay and emergency control, for example fault tolerant strategy, will be examined.

Considering that subjects achieved comparable performances as S2 who had several hours of previous BCI experience, we expect that they would improve their control skills quickly in later studies. Compared to the current EEG-based continuous 2-D BCIs that require months of subject training and may cause fatigue in the long run, the proposed BCI system exhibited prominent advantages. In brief, the results proved the feasibility of the ERD/ERS based brain-controlled virtual wheelchair system, which subjects could rapidly attain a significant level of control with a short calibration period. In the future research, we would consider how to develop asynchronous wheelchair control based on the current system to further increase control speed while maintaining reasonable control accuracy.

REFERENCES

[1] N. Birbaumer, N. Ghanayim, T. Hinterberger, I. Iversen, B. Kotchoubey, A. Kubler, J. Perelmouter, E. Taub, and H. Flor, "A spelling device for the paralysed," *Nature*, vol. 398, pp. 297–298, Mar. 25, 1999.

[2] B. Obermaier, G. R. Muller, and G. Pfurtscheller, ""Virtual keyboard" controlled by spontaneous EEG activity," *IEEE Trans. Neural Syst. Rehabil. Eng.*, vol. 11, no. 4, pp. 422–426, Dec. 2003.

[3] R. M. Jdel, F. Renkens, J. Mourino, and W. Gerstner, "Noninvasive brain-actuated control of a mobile robot by human EEG," *IEEE Trans. Biomed. Eng.*, vol. 51, no. 6, pp. 1026–1033, Jun. 2004.

[4] J. M. Carmena, M. A. Lebedev, R. E. Crist, J. E. O'Doherty, D. M. Santucci, D. F. Dimitrov, P. G. Patil, C. S. Henriquez, and M. A. Nicolelis, "Learning to control a brain-machine interface for reaching and grasping by primates," *PLoS Biol.*, vol. 1, p. E42, Nov. 2003.

[5] M. A. Nicolelis and J. K. Chapin, "Controlling robots with the mind," *Sci. Am.*, vol. 287, pp. 46–53, Oct. 2002.

[6] F. Galan, M. Nuttin, E. Lew, P. W. Ferrez, G. Vanacker, J. Philips, and R. M. Jdel, "A brain-actuated wheelchair: Asynchronous and non-invasive Brain-computer interfaces for continuous control of robots," *Clin. Neurophysiol.*, vol. 119, pp. 2159–2169, Sept. 2008.

[7] M. Velliste, S. Perel, M. C. Spalding, A. S. Whitford, and A. B. Schwartz, "Cortical control of a prosthetic arm for self-feeding," *Nature*, vol. 453, pp. 1098–1101, June 19, 2008.

[8] J. R. Wolpaw, N. Birbaumer, D. J. McFarland, G. Pfurtscheller, and T. M. Vaughan, "Brain-computer interfaces for communication and control," *Clin. Neurophysiol.*, vol. 113, pp. 767–791, Jun. 2002.

[9] C. Mockford, C. Jenkinson, and R. Fitzpatrick, "A review: Carers, MND and service provision," *Amyotroph. Lateral Scler.*, vol. 7, pp. 132–141, Sep. 2006.

[10] M. B. Bromberg, "Quality of life in amyotrophic lateral sclerosis," *Phys. Med. Rehabil. Clin. N Am.*, vol. 19, pp. 591–605, Aug. 2008.

[11] M. T. Williams, J. P. Donnelly, T. Holmlund, and M. Battaglia, "ALS: Family caregiver needs and quality of life," *Amyotroph. Lateral Scler.*, vol. 9, pp. 279–286, Oct. 2008.

[12] M. Mutsaarts, B. Steenbergen, and R. Meulenbroek, "A detailed analysis of the planning and execution of prehension movements by three adolescents with spastic hemiparesis due to cerebral palsy," *Exp. Brain Res.*, vol. 156, pp. 293–304, Jun. 2004.

[13] O. Bai, P. Lin, S. Vorbach, M. K. Floeter, N. Hattori, and M. Hallett, "A high performance sensorimotor beta rhythm-based brain-computer interface associated with human natural motor behavior," *J. Neural Eng.*, vol. 5, pp. 24–35, Mar. 2008.

[14] T. A. Kayagil, O. Bai, C. S. Henriquez, P. Lin, S. J. Furlani, S. Vorbach, and M. Hallett, "A binary method for simple and accurate two-dimensional cursor control from EEG with minimal subject training," *J. Neuroeng. Rehabil.*, vol. 6, p. 14, 2009.

[15] D. Huang, P. Lin, D. Y. Fei, X. Chen, and O. Bai, "Decoding human motor activity from EEG single trials for a discrete two-dimensional cursor control," *J. Neural Eng.*, vol. 6, p. 046005, Aug. 2009.

[16] O. Bai, P. Lin, S. Vorbach, J. Li, S. Furlani, and M. Hallett, "Exploration of computational methods for classification of movement intention during human voluntary movement from single trial EEG," *Clin. Neurophysiol.*, vol. 118, pp. 2637–2655, Dec. 2007.

[17] G. Pfurtscheller and F. H. L. da Silva, "Event-related EEG/MEG synchronization and desynchronization: Basic principles," *Clin. Neurophysiol.*, vol. 110, pp. 1842–1857, Nov. 1999.

[18] R. Leeb and G. Pfurtscheller, "Walking through a virtual city by thought," in *Proc. IEEE Eng. Med. Biol. Soc. Conf*, 2004, vol. 6, pp. 4503–4506.
[19] R. M. J. Del, F. Galan, D. Vanhooydonck, E. Lew, J. Philips, and M. Nuttin, "Asynchronous non-invasive brain-actuated control of an intelligent wheelchair," in *Proc. IEEE Eng. Med. Biol. Soc. Conf.*, 2009, vol. 2009, pp. 3361–3364.
[20] D. J. McFarland and J. R. Wolpaw, "EEG-based communication and control: Speed-accuracy relationships," *Appl. Psychophysiol. Biofeedback*, vol. 28, pp. 217–231, Sep. 2003.
[21] J. R. Wolpaw and D. J. McFarland, "Control of a two-dimensional movement signal by a noninvasive brain-computer interface in humans," *Proc. Nat. Acad. Sci. USA*, vol. 101, pp. 17849–17854, Dec. 21, 2004.
[22] D. J. Krusienski, G. Schalk, D. J. McFarland, and J. R. Wolpaw, "A mu-rhythm matched filter for continuous control of a brain-computer interface," *IEEE Trans. Biomed. Eng.*, vol. 54, no. 2, pp. 273–280, Feb. 2007.
[23] A. S. Royer and B. He, "Goal selection versus process control in a brain-computer interface based on sensorimotor rhythms," *J. Neural Eng.*, vol. 6, p. 016005, Feb. 2009.
[24] A. S. Royer, A. J. Doud, M. L. Rose, and B. He, "EEG control of a virtual helicopter in 3-dimensional space using intelligent control strategies," *IEEE Trans. Neural Syst. Rehabil. Eng.*, vol. 18, no. 6, pp. 581–589, Dec. 2010.
[25] G. Vanacker, R. M. J. Del, E. Lew, P. W. Ferrez, F. G. Moles, J. Philips, H. Van Brussel, and M. Nuttin, "Context-based filtering for assisted brain-actuated wheelchair driving," *Comput. Intell. Neurosci.*, p. 25130, 2007.
[26] C. J. Bell, P. Shenoy, R. Chalodhorn, and R. P. Rao, "Control of a humanoid robot by a noninvasive brain-computer interface in humans," *J. Neural Eng.*, vol. 5, pp. 214–220, Jun. 2008.
[27] H. K. Kim, S. J. Biggs, D. W. Schloerb, J. M. Carmena, M. A. Lebedev, M. A. Nicolelis, and M. A. Srinivasan, "Continuous shared control for stabilizing reaching and grasping with brain-machine interfaces," *IEEE Trans. Biomed. Eng.*, vol. 53, no. 6, pp. 1164–1173, Jun. 2006.
[28] D. J. McFarland, W. A. Sarnacki, and J. R. Wolpaw, "Electroencephalographic (EEG) control of three-dimensional movement," *J. Neura. Eng.*, vol. 7, p. 036007, Jun. 2010.
[29] Y. Li, J. Long, T. Yu, Z. Yu, C. Wang, H. Zhang, and C. Guan, "An EEG-based BCI system for 2-D cursor control by combining Mu/Beta rhythm and P300 potential," *IEEE Trans. Biomed. Eng.*, vol. 57, no. 10, pp. 2495–2505, Oct. 2010.
[30] P. Sykacek, S. Roberts, M. Stokes, E. Curran, M. Gibbs, and L. Pickup, "Probabilistic methods in BCI research," *IEEE Trans. Neural Syst. Rehabil. Eng.*, vol. 11, no. 2, pp. 192–195, Jun. 2003.
[31] N. Birbaumer, "Breaking the silence: Brain-computer interfaces (BCI) for communication and motor control," *Psychophysiology*, vol. 43, pp. 517–532, Nov. 2006.
[32] G. Pfurtscheller, "Functional topography during sensorimotor activation studied with event-related desynchronization mapping," *J. Clin. Neurophysiol.*, vol. 6, pp. 75–84, Jan. 1989.
[33] G. Magnani, M. Cursi, L. Leocani, M. A. Volonte, T. Locatelli, A. Elia, and G. Comi, "Event-related desynchronization to contingent negative variation and self-paced movement paradigms in Parkinson's disease," *Mov. Disord.*, vol. 13, pp. 653–660, Jul. 1998.
[34] W. Szurhaj, E. Labyt, J. L. Bourriez, F. Cassim, L. Defebvre, J. J. Hauser, J. D. Guieu, and P. Derambure, "Event-related variations in the activity of EEG-rhythms. Application to the physiology and the pathology of movements," *Epileptic Disord.*, pp. 59–66, Jul. 2001.
[35] G. Pfurtscheller and T. Solis-Escalante, "Could the beta rebound in the EEG be suitable to realize a "brain switch"?," *Clin. Neurophysiol.*, vol. 120, pp. 24–29, Jan. 2009.
[36] H. H. Jasper and H. L. Andrews, "Electro-encephalography. III. Normal differentiation of occipital and precentral regions in man," *Arch. Neurol. Psychiat.*, vol. 39, pp. 95–115, 1938.
[37] R. Simpson, E. Lopresti, S. Hayashi, I. Nourbakhsh, and D. Miller, "The smart wheelchair component system," *J. Rehabil. Res. Develop.*, vol. 41, pp. 429–442, May 2004.
[38] B. Hjorth, "An on-line transformation of EEG scalp potentials into orthogonal source derivations," *Electroencephalogr. Clin. Neurophysiol.*, vol. 39, pp. 526–530, Nov. 1975.
[39] P. L. Nunez, R. Srinivasan, A. F. Westdorp, R. S. Wijesinghe, D. M. Tucker, R. B. Silberstein, and P. J. Cadusch, "EEG coherency. I: Statistics, reference electrode, volume conduction, Laplacians, cortical imaging, and interpretation at multiple scales," *Electroencephalogr. Clin. Neurophysiol.*, vol. 103, pp. 499–515, Nov. 1997.
[40] G. Pfurtscheller, "Mapping of event-related desynchronization and type of derivation," *Electroencephalogr. Clin. Neurophysiol.*, vol. 70, pp. 190–3, Aug. 1988.
[41] M. T. Elliott, A. E. Welchman, and A. M. Wing, "MatTAP: A MATLAB toolbox for the control and analysis of movement synchronisation experiments," *J. Neurosci. Methods*, vol. 177, pp. 250–257, Feb. 2009.
[42] A. Chatterjee, V. Aggarwal, A. Ramos, S. Acharya, and N. V. Thakor, "A brain-computer interface with vibrotactile biofeedback for haptic information," *J. Neuroeng. Rehabil.*, vol. 4, p. 40, 2007.
[43] T. Fawcett, ROC Graphs: Notes and practical considerations for data mining researchers 2003.
[44] R. Leeb, F. Lee, C. Keinrath, R. Scherer, H. Bischof, and G. Pfurtscheller, "Brain-computer communication: Motivation, aim, and impact of exploring a virtual apartment," *IEEE Trans. Neural Syst. Rehabil. Eng.*, vol. 15, no. 4, pp. 473–482, Dec. 2007.
[45] D. J. McFarland, W. A. Sarnacki, T. M. Vaughan, and J. R. Wolpaw, "Brain-computer interface (BCI) operation: Signal and noise during early training sessions," *Clin. Neurophysiol.*, vol. 116, pp. 56–62, Jan. 2005.

Dandan Huang received the B.S. degree in biomedical engineering from Tianjin University, Tianjin, China, in 2007, and the M.S. degree, in 2009, from Virginia Commonwealth University, Richmond, where she is currently working toward the Ph.D. degree in biomedical engineering.

Her research interests include brain–computer interface, rehabilitation robotics, and machine learning.

Kai Qian received the B.S. degree in automatic control from the East China University of Science and Technology, Shanghai, China, in 2005, and the M.S. degree in biomedical engineering from Virginia Commonwealth University, Richmond, in 2010. He is currently working toward the Ph.D. degree in the Department of Biomedical Engineering, Illinois Institute of Technology, Chicago.

His research interests include sensorimotor control of hand, rehabilitation robotics, and brain–machine interface.

Ding-Yu Fei (M'98) graduated from Tsinghua University, Beijing, China, in electronic engineering, in 1965, and received the Ph.D. degree in bioengineering from Pennsylvania State University, College Park, in 1986.

He is currently an Associate Professor and Director of Biomedical Instrumentation and Medical Imaging Laboratories in Department of Biomedical Engineering at Virginia Commonwealth University, Richmond. His research interests include applications of biomedical instrumentation in telemedicine and brain–computer interface, and applications of medical imaging technologies in cardiovascular systems.

Wenchuan Jia received the B.E., M.E. and Ph.D. degrees in mechatronics from Huazhong University of Science and Technology, Wuhan, China, in 2003, 2006, and 2011, respectively.

He has been a Lecturer in the School of Mechatronic Engineering and Automation, and Shanghai Key Laboratory of Manufacturing Automation and Robotics, Shanghai University (SHU), Shanghai, China. His current research interests include biomimetic control, legged robots, and dynamical simulation.

Xuedong Chen received the B.S. and M.S. degrees in mechanical engineering from Wuhan University of Technology, Wuhan, China, in 1984 and 1989, and the Ph.D. degree from Saga University, Japan, in 2001.

He has been a Professor in the School of Mechanical Science and Engineering, Huazhong University of Science and Technology, Wuhan, China. He serves as the Vice Director of the State Key Laboratory of Digital Manufacturing Equipment and Technology. His research interests include mechanical dynamics, intelligent robots, and mechatronics.

Ou Bai received the B.S. degree in electronic engineering from Tsinghua University, Beijing, China, in 1991, and the Ph.D. degree from Saga University, Saga, Japan, in 2000.

He worked in National Institute of Neurological Disorders and Stroke/National Institutes of Health as a Postdoctoral Fellow from 2002 to 2007 before he joined the Department of Biomedical Engineering at Virginia Commonwealth University, Richmond, as an Assistant Professor. He serves as the Director of EEG&BCI Lab. His current research interests include human motor control neurophysiology, brain–computer interfaces, and neurorehabilitation.